NASA CONTRACTOR REPORT

NASA CR-38

NASA CR-386

AN INVESTIGATION OF SUPERCONDUCTIVE TECHNIQUES FOR BROADBAND TRAVELING-WAVE MASERS

Prepared under Contract No. NAS 5-3773 *by*
RADIO CORPORATION OF AMERICA
Camden, N. J.
for Goddard Space Flight Center

NATIONAL AERONAUTICS AND SPACE ADMINISTRATION • WASHINGTON, D. C. • MARCH 1966

NASA CR-386

AN INVESTIGATION OF SUPERCONDUCTIVE TECHNIQUES FOR BROADBAND TRAVELING-WAVE MASERS

Prepared under Contract No. NAS 5-3773 by
RADIO CORPORATION OF AMERICA
Camden, N. J.

for Goddard Space Flight Center

NATIONAL AERONAUTICS AND SPACE ADMINISTRATION

For sale by the Clearinghouse for Federal Scientific and Technical Information
Springfield, Virginia 22151 – Price $2.00

ABSTRACT

Research conducted with multicoil superconducting magnets capable of operating with traveling-wave masers is described. The experimental work performed was confined to double- and triple-field stagger tuning of a rutile meander-line traveling-wave maser; these measurements are compared with the theory for broadbanding traveling-wave masers. A technique for obtaining extremely wide bandwidth (120 Mc) in masers is presented.

As a result of this project, traveling-wave masers with bandwidths exceeding 200 Mc may be developed immediately, using presently available materials and techniques. It is also shown that experimental traveling-wave masers capable of trading gain for bandwidth electronically may be designed.

Since the theory of magnetic stagger tuning for increased bandwidth has been established, it is recommended that continued research be conducted in the areas of improved rutile crystal performance and optimum loadings of the meander-line rutile maser. All indications point to traveling-wave maser bandwidths of 20 per cent to be fully realizable in the near future.

TABLE OF CONTENTS

Section I

INTRODUCTION

Since the inception of the traveling-wave maser,[1] a considerable improvement in performance has occurred. Where the initial work with traveling-wave masers was conducted at 1.7 ^{o}K bath temperature, reliable high-gain amplifiers are now consistently designed at 4.2 ^{o}K. Operational amplifiers at bath temperatures of 15 to 20 ^{o}K have been reported.[2] Essentially, large gains per inch have resulted in traveling-wave masers with gains far in excess of what might be conveniently employed with an ultra-low-noise microwave receiving system. The logical direction to follow is to exchange this gain for bandwidth. This problem of gain/bandwidth trading has been studied by a number of workers.[3,4] In almost all of these cases stagger tuning of the resonance line has been the method of accomplishing this gain/bandwidth tradeoff. This method employed shaping the pole faces of permanent and rather heavy laboratory magnets. The purpose of this research program is to find ways of providing this shifting (or staggering) of the resonance line in a more convenient manner with a superconducting magnet to establish a criterion for developing superconducting magnets that are capable of providing the magnetic field profile for extremely wide bandwidth masers. This research centers around the multicoil superconducting magnet as a mechanism for achieving this end. Since gain and bandwidth may be traded electronically from a remote control center, and the packaging of a lightweight maser system may be more readily achieved with the superconducting magnet, this approach is a logical one to pursue.

The purpose of this research and report is to show how superconducting magnets may be employed towards this end. The purpose of this program is to verify the feasibility of multicoil magnetic stagger tuning in conjunction with superconducting magnetic design as being the most sophisticated method of accomplishing large bandwidth amplification.

This report describes a novel superconducting magnet design employing superconducting shields to contain the magnetic flux and six variable magnetic fields to allow for resonance linewidth broadening. In order to verify the existing theory on magnetic stagger tuning established by Ostermeyer,[3] it was necessary to develop a high-gain traveling-wave maser. An iron-doped rutile maser operating at 4.0 Gc was chosen for this purpose. Since the actual performance of the magnet can be correlated only against the efficiency with which gain is traded for bandwidth in an operational traveling-wave maser, a considerable number of maser experiments were conducted and the comparison as to gain/bandwidth exchange was made.

Three sections of the six-coil superconducting magnet were employed. It is felt that the utilization of superconducting magnets as a mechanism for achieving this trade has been shown and that masers with bandwidths far in excess of those reported in this report may be developed.

Section II

SUPERCONDUCTING MAGNET CONSIDERATIONS

A. MAGNET DESIGN AND FABRICATION

It has been shown that the transverse magnetic field for a traveling wave maser can be most economically provided by a superconducting electromagnet in which leakage and fringing flux are almost entirely eliminated by a superconducting shield. Under these conditions, the electromagnet operates with very high efficiency because it is required to develop only the air gap flux. Furthermore, the absence of fringing flux across the air gap assures a high degree of field uniformity. A typical magnetic circuit configuration is shown in Figure 1. The magnet is a symmetrical structure consisting of a pair of pole pieces. The height and width of the pole faces are determined by the volume over

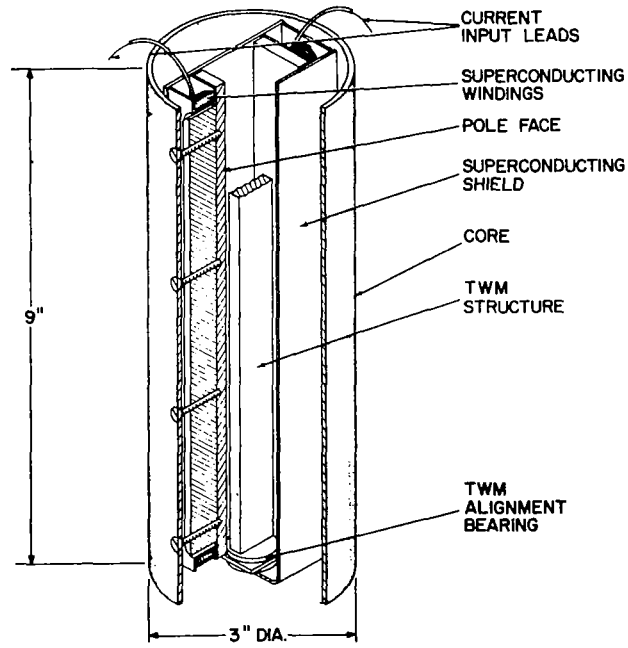

Figure 1. Cross-section of Superconducting Magnet and Traveling-Wave Maser

which a uniform field must be supplied. The total magnetic circuit flux is developed by exciting superconducting windings wound around cores on opposite sides of the air gap. The magnetic circuit is completed through the external core. The latter is preferably cylindrical for simplicity and precision in machining. The superconducting shield extends the full length of the pole faces and air gap to eliminate fringing flux across the air gap.

A field uniformity of approximately one oersted in 5000 requires comparable mechanical precision in the mechanical configuration of the electromagnet. Since the normally fringing flux within the air gap follows the contour of the superconducting enclosure, the latter must be in intimate contact and conform accurately to the contour of the pole pieces.

The materials of the magnetic circuit are chosen for optimum performance to reduce the size and weight of the mass to be cooled. High permeability materials are employed since elimination of fringing air gap flux by means of superconducting shields does not by itself assure uniformity of air gap field (unless the pole pieces are equipotential surfaces). The 45 permalloy (45 per cent nickel, 55 per cent iron) material such as 4750 Allegheny alloy, with saturation density of 15,500 gauss, is well suited for this application because it can be operated with a permeability of approximately 10,000 at a flux density of 13,000 gauss. The material is ductile and can be readily machined. The desirable magnetic characteristics are developed by heat treatment above $1000^{o}C$ for several hours in an atmosphere of pure dry hydrogen. The pole face surfaces are subsequently ground, to eliminate distortion resulting from this heat treatment, followed by a strain anneal at a temperature of $600^{o}C$.

It is generally desirable to make the core integral with the pole pieces except in cases where it is necessary to reduce the size of the core by using a material having a higher flux density than the material of the poles. In this event the appropriate material for the core is Permendur, an alloy of 50 per cent iron and 50 per cent cobalt with saturation density of 24,500 gauss. This material can be

operated at a flux density of 20,000 gauss with a permeability of approximately 4000. The material is brittle but can be machined without difficulty. The optimum magnet characteristics are developed by heat treatment at approximately 880°C in pure dry hydrogen.

The cylindrical return circuit (or external core) is made of mild steel. It is heat treated at 1000°C in pure dry hydrogen with slightly undersize inside diameter and is subsequently ground to final dimensions.

The electromagnet is required to develop a magnetomotive force equal to the sum of the magnetomotive force drops across the air gap and the magnetic materials of the magnetic circuit. In the conventional magnetic circuit the increase in effective length of air gap due to the fringing field must also be taken into account. For the configuration discussed here, however, the parts of the magnetic circuit are chosen to operate at high permeability and high flux density with negligible magnetomotive force drop in the magnetic material. Also, in the absence of fringing field due to the action of the superconducting shield, the pole separation is the actual air gap length ℓ_g. Consequently, where B_g is the air gap flux density, the magnetomotive force can be expressed simply as

$$F = B_g \ell_g = n i$$

Expressed in convenient units, it is easily shown that

$$B_g = \frac{0.5\, n\, i}{\ell_g} ,$$

where

- n is the total number of turns,
- i is the current in amperes,
- ℓ_g is the gap opening in inches, and
- B_g is the gap flux in gauss.

This simple equation is extremely useful in quickly determining magnet design parameters.

B. SUPERCONDUCTING SHIELDS

A first approach to achieving field shaping with superconductors is to determine the ability of various metals to repel a magnetic field from its interior. The field penetration into hard superconductors is quite different from soft superconductors (London model[5]) and is only recently becoming understood. The results reported here mark the first definitive measurements that allow a prediction of the field which can be contained by a given thickness of superconductor.

In the usual design of iron-core superconducting magnets for traveling-wave masers, described in more detail in the previous section, a high-saturation ferromagnetic material is carefully machined into a cylindrical cyclotron-type configuration with long (7 to 8 inches) pole pieces. Fine (0.005 inch) NbZr superconducting wire is then wound on the pole pieces to supply a large magnetomotive force. Rectangular pole faces are precision ground from a high-permeability material and attached to the pole pieces in parallel alignment to ensure a constant gap length. A U-shaped superconducting foil is placed around the pole faces, thereby enclosing the gap space on three sides. The top is left open to insert the traveling-wave maser.

As the field in the gap space is increased, the fringing field is eliminated by the diamagnetic screening currents which are induced in the superconducting foil. Presumably, the foil acts to concentrate the flux, the spatial homogeneity resulting from the mutually repulsive action of the lines. When the screening current in the foil reaches its maximum value, the flux begins to "leak" out and the field is no longer proportional to the current. If this phenomenon occurs gradually (no flux jumps), the field remains homogeneous but does not increase significantly beyond this saturation value.

Careful measurements have been carried out to determine the saturation field, B_{sat}, of a given superconductor and how this value increases with increasing foil thickness. Figures 2 and 3 present the final results of this phase of the program. These curves are taken from X-Y recorder plots using a sensitive Hall probe[6] placed in the center of the gap space. Measurements with the traveling-wave maser

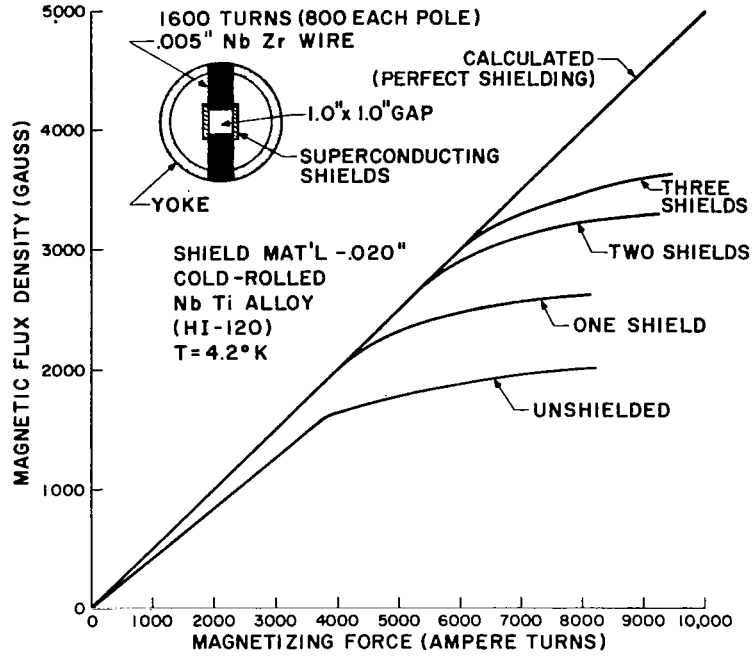

Figure 2. Dependence of Saturation Field of NbTi Superconducting Foil on Foil Thickness

show that the field generated by these superconducting magnets is at least as spatially homogeneous as that produced by a standard 12-inch laboratory magnet. This conclusion is based on the absence of artificial broadening of the paramagnetic resonance line which is caused by an inhomogeneous dc magnetic field. Determination of the linewidth of Fe^{+3}:TiO_2 using superconducting magnets yields the same value reported previously when using standard laboratory magnets of high homogeneity.[7] The material used in the RCA measurements is a niobium-titanium alloy, the most favorable superconductor presently known for this application. This investigation also pointed out that in spite of its higher critical current, the niobium-zirconium alloy is not as suitable due to the instability of the screening currents which results in flux jumps. Figure 3 presents the curves obtained for niobium-zirconium foils.

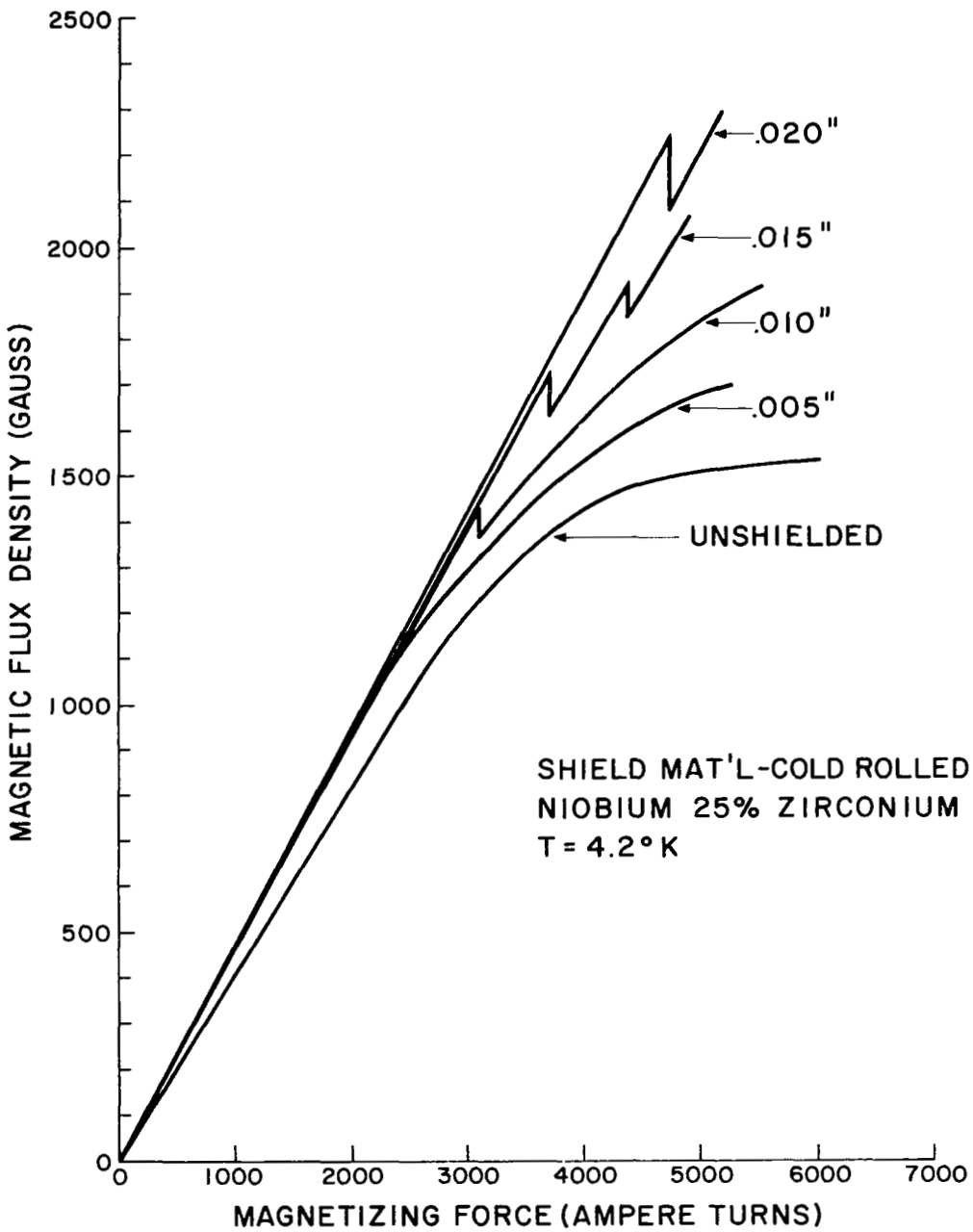

Figure 3. Dependence of Saturation Field of NbZr Superconducting Foil on Foil Thickness

C. STAGGER TUNING WITH SUPERCONDUCTING MAGNET

The use of magnetic shielding to obtain uniform fields over considerable structure lengths has already been discussed. This section describes how magnetic step variations can be accomplished along the maser. The sketch in Figure 4 schematically shows the principles involved and the configuration of a magnet.

The cores consist of solid cylinders made from a high-saturation ferromagnetic material (Permendur, $B_m \approx 24,000$ gauss). They are magnetized by high current superconducting windings (0.010-inch Nb-25% Zr). The gap field is proportional to the quantity ni, so that the current can be adjusted to generate the desired field, i.e., $H_1 \propto n_1$, $H_2 \propto n_2$, etc.

The magnet is fabricated with an equal number of windings on each pole; the exact number of the ampere turns required for each crystal can be experimentally

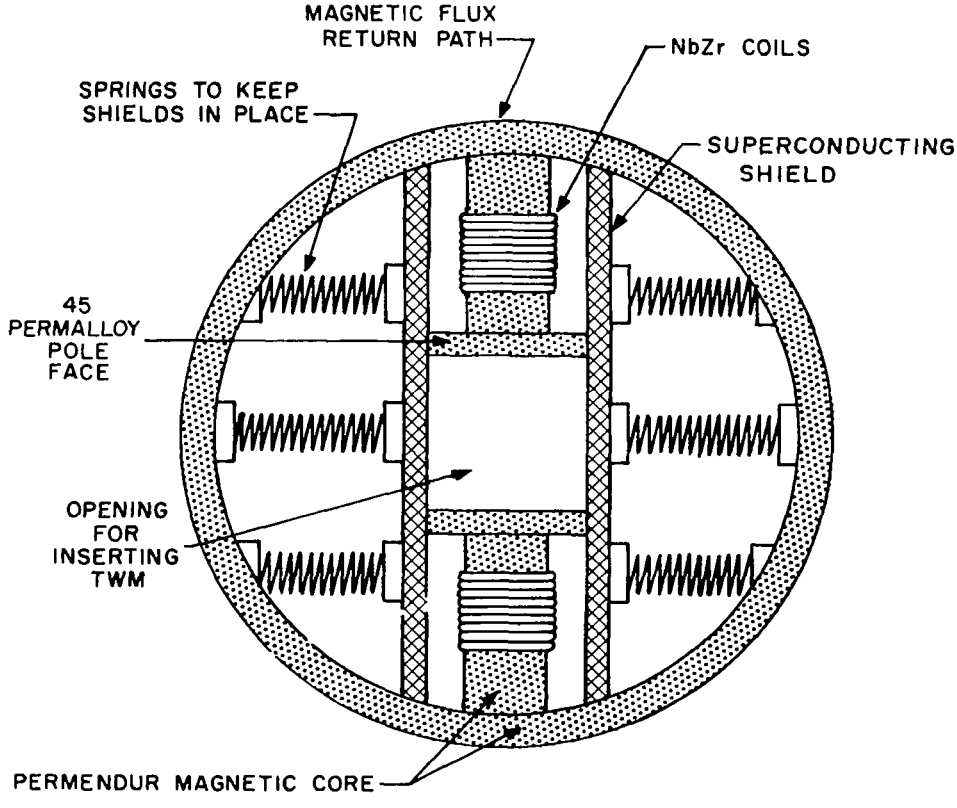

Figure 4. Configuration of Superconducting Magnet Used for Stagger Tuning

determined. When the final design is begun, the number of turns for each pole can be adjusted so that a series current can be used to generate the required field variation. This type of operation will allow the amplified band to be tuned by a single adjustment of the magnet current. A series coil also provides persistent current operation. Individual parallel windings with the same number of turns can provide stagger tuning by proper adjustment of the current levels in each winding. Series connection of the windings with superconducting joints (easily accomplished by spot-welding onto a hard superconducting tab) provides a standard (unstaggered) field that can be used for conventional maser operation from 0-4 kilogauss. Table I points out the unique property and function of each material used in the fabrication of this magnet.

The magnet just described has been used as a prototype for the stagger-tuning device.

TABLE I. PROPERTIES AND FUNCTIONS OF SUPERCONDUCTING MAGNET MATERIALS

Material	Property	Function
NbZr	High critical current.	Magnetizing windings.
Vapor-deposited Nb_3Sn	High critical field; high critical current; can be deposited in strips.	Magnetic insulator between field steps; shield around air gap to prevent fringing.
Permendur	High saturation magnetization.	Magnetic core with minimum volume.
45 Permalloy	High permeability at 2-3 kgauss.	Pole faces with equipotential surface.

Section III

TRAVELING-WAVE MASER CONSIDERATIONS

A. DESIGN CRITERIA

The design of wide bandwidth masers (that is, amplifiers with bandwidth exceeding 5 per cent) requires optimum gain performance from the traveling-wave maser, since gain is subsequently traded for bandwidth. Essentially the optimum in maser filling factor and isolator design is required, along with the maximum in inversion ratio. The larger the crystal linewidth, the greater the exchange of gain for bandwidth, provided these other factors remain constant. Ideally one wants a high inversion ratio, large paramagnetic susceptibility χ'' and large crystal linewidth.

Table II shows how the three most common maser materials perform with relation to the most important parameters.

TABLE II. CHARACTERISTICS OF MASER MATERIALS

Material	Gain/Bandwidth Tradeoff	Inversion Ratio at 4 Gc	Linewidth (Mc)	$Q_m = K(\chi'')$	Magnetic Field (kilogauss)
Ruby Cr^{+3} (Al_2O_3)	1 db = 1 Mc	3 to 1	57	125	3.3
Rutile Cr^{+3}:TiO_2	3 db = 1 Mc	10 to 1	20	50	3.0
Rutile Fe^{+3}:TiO_2	1 db = 1 Mc	13 to 1	58 (c-axis) 70 (a-axis)	50	2.5

Table II indicates iron-doped rutile to be the best choice since its characteristics are superior. In addition, the lower magnetic field requirements allow for the construction of a smaller and lighter superconducting magnet.

In order to achieve maximum gain and consequently maximum bandwidth, it is desirable to have constant high slowing over the desired operating range. The dispersion characteristics for the meander line slow wave circuit loaded with rutile indicate that for a 5 per cent bandwidth and an optimum filling factor, a slowing $\left(\frac{\partial \omega}{\partial \beta} / c\right)$ of 75 may be achieved.

Since the dielectric loading and dispersion characteristics for iron-doped rutile are the same as chromium-doped rutile when loaded on a meander-line slow-wave circuit, the design of a 4.0-Gc amplifier followed the same lines previously employed at S-band.[8] Since the iron requires a low dc magnetic field, the shape factor for the reverse isolator required adjustment.

Small rectangular chips of 10 per cent gadolinium-substituted YIG provided excellent isolation across the desired operating band, and reverse isolation greater than 150 db was achieved, assuring extreme stability. The isolator figure of merit measured 20-to-1, and less than 8 db forward loss was contributed by the isolator alone. The experimental amplifier employed 4.0 inches of active crystal, and electronic gains of approximately 20 db per inch were achieved. The total loss per inch measured 4 db, two db as a result of copper and matching losses and 2 db as a result of the forward ferrite losses. This maser was easily pump-power saturated and was found to be quite stable. With an electronic gain of 78 db and a bandwidth of 12 Mc (tunable over a 200-Mc range), it was felt that a device was now available with sufficient performance that gain could be traded for bandwidth.

B. DOUBLE-FIELD STAGGER TUNING

To provide the proper magnetic fields for double-field stagger tuning, Sections 1 and 2 of the magnet (Figures 5 and 6) were connected in series and placed across a highly regulated current supply. Sections 3, 4, 5 and 6 were similarly connected, providing two individually variable magnetic fields of high uniformity. The paramagnetic crystal (Fe^{+3}: TiO_2) was divided in half, as shown in Figure 7. The crystal halves were placed in two separate magnetic fields and tuned to resonate at different frequencies.

As the two resonant frequencies were separated, the gain-vs-frequency curve, at first, simply appeared to broaden. However, as the separation was increased, the gain-vs-frequency curve became double-humped with a depression in the center and, consequently, a minimum appeared in the passband.

The instantaneous response was determined at various values of Δf_m, the separation between the resonant frequencies. Figure 8 shows smooth curves drawn through experimental points obtained by measuring the electronic gain at 10-Mc intervals, the pump frequency being tuned at each signal setting to ensure pump saturation. The traveling-wave maser was gain-stabilized with greater than 150 db of reverse isolation. The reverse isolator was an integral part of the slow-wave circuit. Broadbanding was achieved by keeping the current fixed in the top set of coils (resonant frequency 3988 Mc) and setting the current in the bottom set of coils at increasingly higher values. Table III lists the important parameters of the measurements plotted in Figure 8. The center frequency, f_o, has been recorded along with G_p, the peak electron gain; Δf, the instantaneous 3-db bandwidth; ΔI_m, the current difference in the magnetic coils; Δf_m, the difference between the resonant frequencies, and Δf_L, the natural linewidth of the crystal.

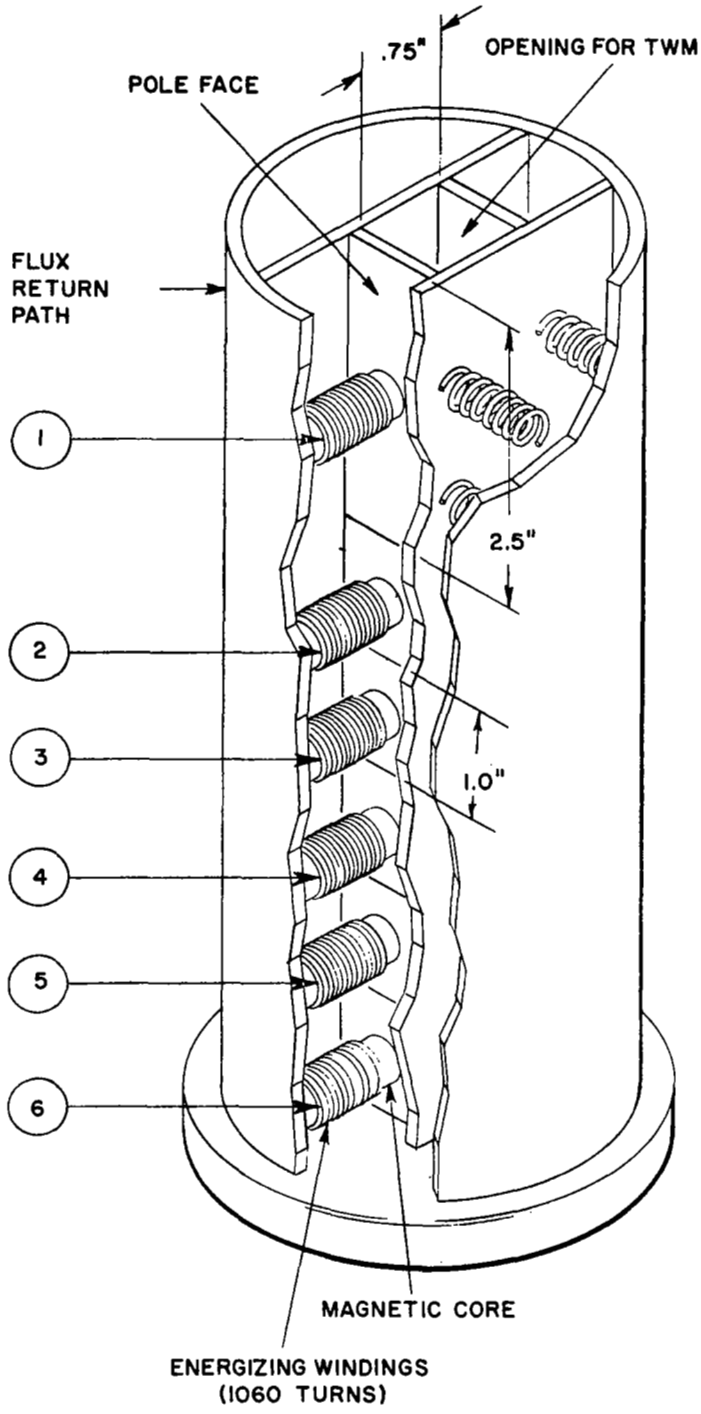

Figure 5. Cutaway View of Lower Portion of Six-Stage Superconducting Magnet

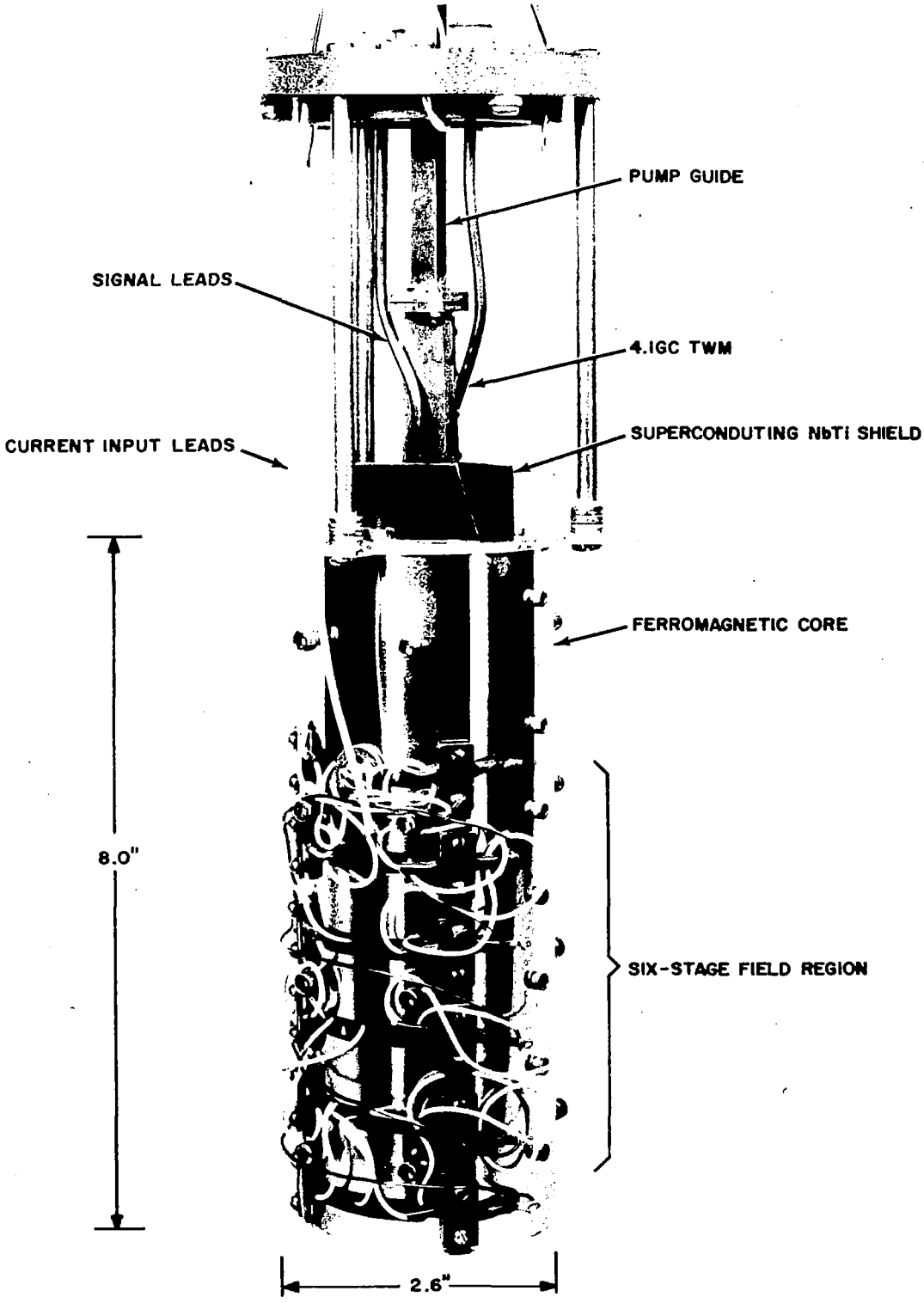

Figure 6. Photograph of Six-Stage Superconducting Magnet

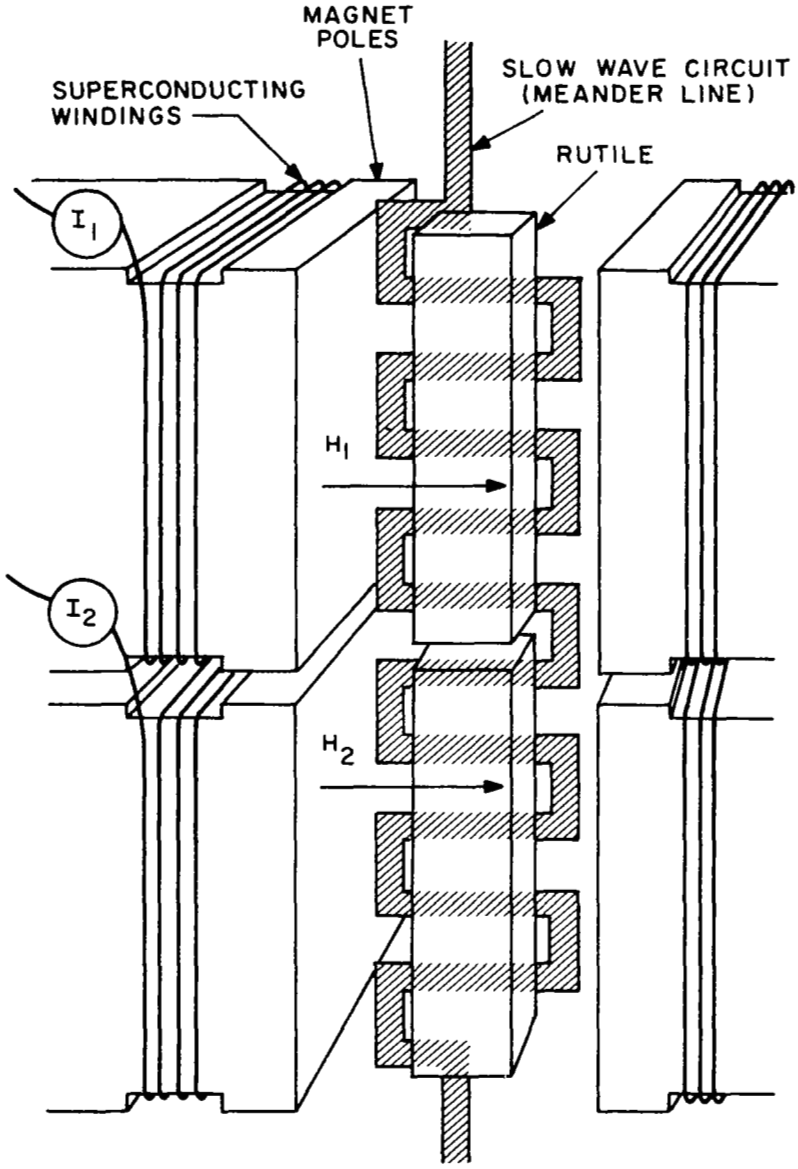

Figure 7. Double-Field Stagger-Tuning of Traveling-Wave Maser

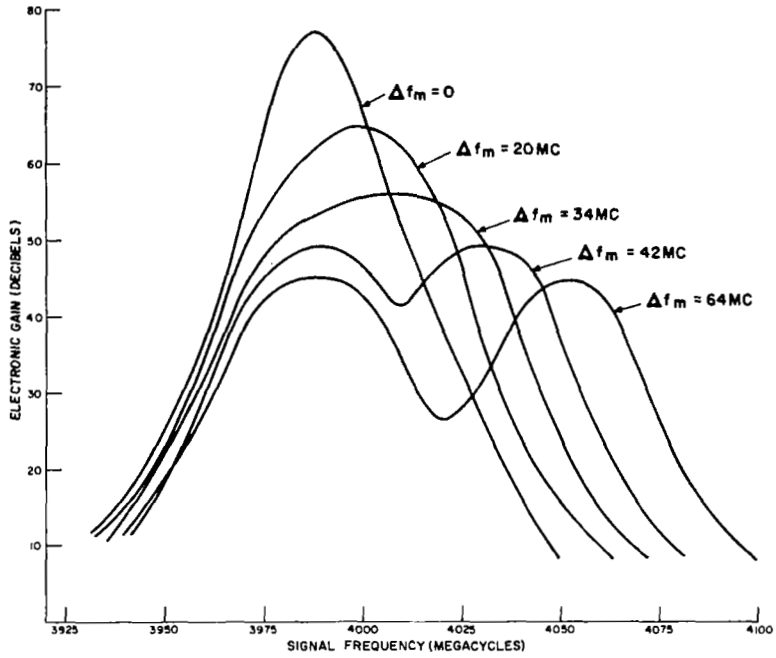

Figure 8. Experimental Gain-Frequency Response of Stagger-Tuned Traveling-Wave Maser

TABLE III. EXPERIMENTAL DATA ON STAGGER-TUNED TRAVELING-WAVE MASER

f_o (Mc)	Δf_m (Mc)	$\Delta f_m/\Delta f_L$	ΔI_m (A)	G_p (db)	Δf (Mc)
3988	0	0	0	77	12
3998	20	0.333	—	65	22
4005	34	0.567	0.02	56	38
4009	42	0.700	—	49*	+
4020	64	1.06	0.04	45*	+

* Gain at resonant peaks.
\+ Gain ripple greater than 3 db.

Theoretically, the electronic gain (in db) of a traveling-wave maser is given by

$$G_{db} = 27.3 \frac{FS\ell}{\lambda_o} \chi'' \qquad (1)$$

where

F = filling factor,

S = slowing = ν_g/c or $\frac{\partial\omega/\partial\beta}{c}$,

ℓ = physical length of the paramagnetic material,

λ_o = free space wavelength of the signal,

χ'' = the imaginary part of the paramagnetic susceptibility.

Because each term is approximately independent of frequency over a 100-Mc band, the instantaneous response of the maser amplifier is determined by the paramagnetic susceptibility. Typically, Lorentzian line shapes have been used for χ'' since the expressions are simple and found to be in reasonable agreement with experimental line shapes. The frequency-dependent gain expression can be written

$$G_{db}(f) = 27.3\,\frac{FS\ell}{\lambda_o}\,\frac{\chi\delta''}{1+\left[2\,(f-f_m)/\Delta f_L\right]^2} = \frac{G_o}{1+\left[2\,(f-f_m)/\Delta f_L\right]^2} \tag{2}$$

where

f_m is the magnetic resonance frequency,

f is the signal frequency,

χ_o'' is the maximum value of susceptibility, and

G_o is the electronic gain at resonance; i.e., where $f=f_m$.

If the paramagnetic crystal has uniform electronic properties and is divided into two equal lengths, Equation 2 becomes

$$G_{db}(f) = \frac{G_o}{2}\left[\frac{1}{1+\left[2\,(f-f_o-\Delta f_m/2)/\Delta f_L\right]^2} + \frac{1}{1+\left[2\,(f-f_o+\Delta f_m/2)/\Delta f_L\right]^2}\right] \tag{3}$$

where

f_o is the center frequency.

By properly manipulating Equation 3, it can be shown that there is a well-defined point at which ripple in the gain curve is just detectable. This is the "optimally flat" point and constitutes maximum performance of the traveling-wave maser. Theoretically, this condition occurs when the separation between the resonant frequencies reaches $\Delta f_m = 0.577\ \Delta f_L$. According to this result, the experimental curve shown for $\Delta f_m = 34$ Mc (Figure 8) is very close to the optimally flat point. Note that in this case the gain is reduced to 56/77 = 73 per cent of the unstaggered value, within one per cent of the theoretical value, and the instantaneous 3-db bandwidth is 38 Mc.

Figure 9 is a theoretical plot of the gain equation for this "nearly flat" point, where $f_o = 4005$ Mc, $\Delta f_m = 34$ Mc and $G_o = 77$ db. The circles represent the experimental points. Note that the gain data has not been normalized but, rather, has been set to its value at resonance, $\Delta f_m = 0$. This is strong evidence that the maser is not being degraded by the staggered field.

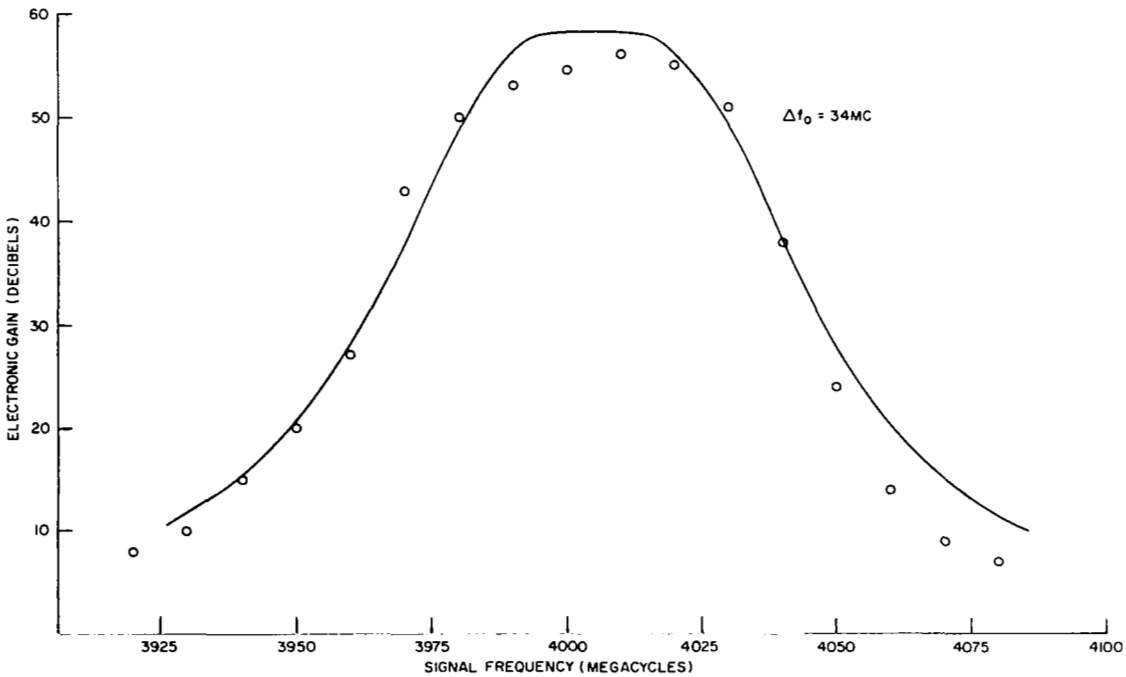

Figure 9. Comparison of Experimental Results with Lorentzian Line Shape Near Optimally Flat Point

C. TRIPLE FIELD STAGGERING

1. Graphic Analysis

The maximum bandwidth that can be obtained from double-field staggering of the four-inch Fe^{+3}: TiO_2 traveling-wave maser has been shown to be 38 Mc. The next step in the stagger-tuning program is to determine the maximum bandwidth that can be obtained using three separate magnetic fields. Again it must be noted that the experiments (and, consequently, the analysis associated with those experiments) were carried out with only 4 inches (two 2-inch pieces) of crystal. Thus, before the crystals were cut, some graphic analysis was necessary to determine the optimum size of each piece of crystal.

In triple-field staggering, the center section receives gain contributions from each of the other two sections and thus must be shorter in length than the side crystals in order to yield a flat response. There are then two ratios that determine the over-all gain/frequency response of the stagger-tuned traveling-wave maser:

$$\alpha = \frac{\ell_c}{\ell_s} \quad \text{and} \quad \beta = \frac{\Delta f_o}{\Delta f_L} \quad ,$$

where

α determines the relative length of the crystal pieces,

β determines the spacing between the resonant frequencies,

ℓ_c is the length of the center crystal in inches,

ℓ_s is the length of the side crystals in inches,

Δf_o is the separation between resonant frequencies in megacycles,

Δf_L is the natural linewidth of paramagnetic resonance (megacycles).

In order to approximate the optimum value of these ratios for triple-field staggering, two values of α were chosen and the resulting gain/bandwidth was investigated for several values of β. Table IV gives the values of the peak electronic gain of the center and side sections of the stagger-tuned traveling-wave maser.

TABLE IV. OVER-ALL GAIN RESPONSE FOR VARIATIONS IN CRYSTAL LENGTH

α	ℓ_s (in)	G_{ps} (db)	ℓ_c (in)	G_{pc} (db)
0.67	1.50	29.25	1.00	19.5
0.75	1.455	28.40	1.091	21.3

Figure 10 gives the response of the four-inch traveling-wave maser for an α value of 0.67. Figure 11 shows the result for $\alpha = 0.75$. It can be seen that the response for $\alpha = 0.67$ and $\beta = 0.583$ is close to optimum for achieving a flat gain/frequency curve, i.e., a minimum of ripple. These curves are based on Lorentzian line shapes, using a value of 60 Mc for the natural linewidth.

The above theoretical results have been tested in the superconducting magnet energized so as to produce three separate magnetic fields. As shown in

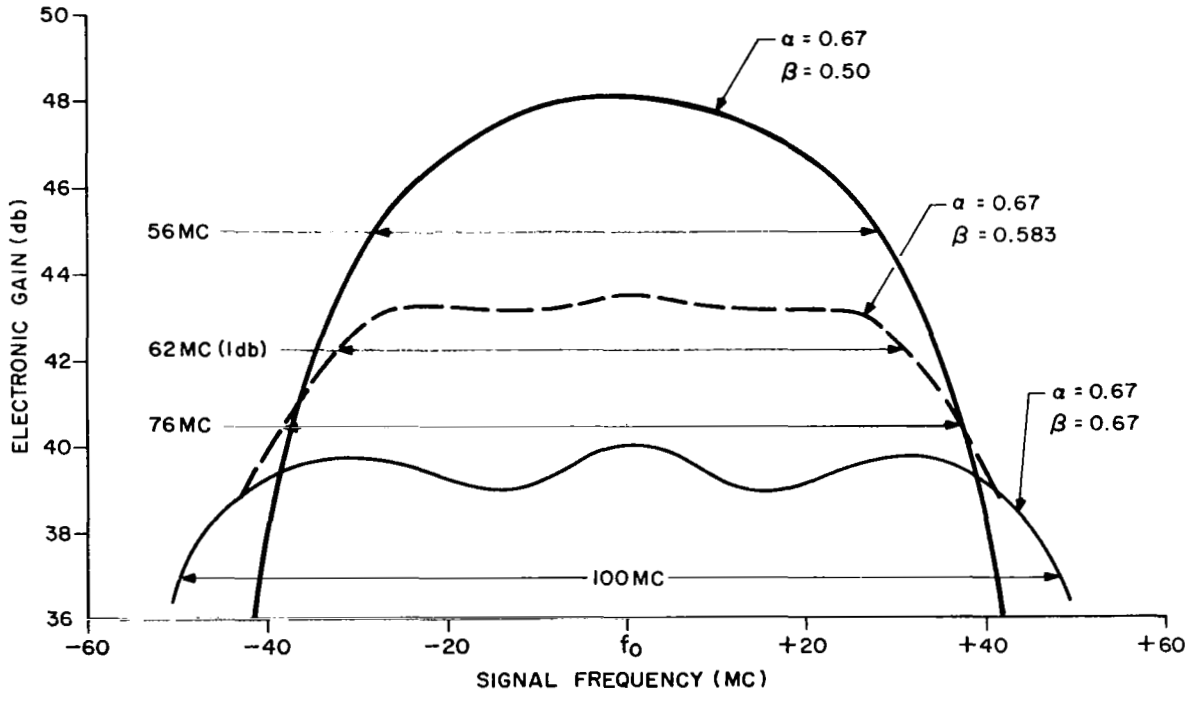

Figure 10. Gain and Bandwidth for $\alpha = 0.67$

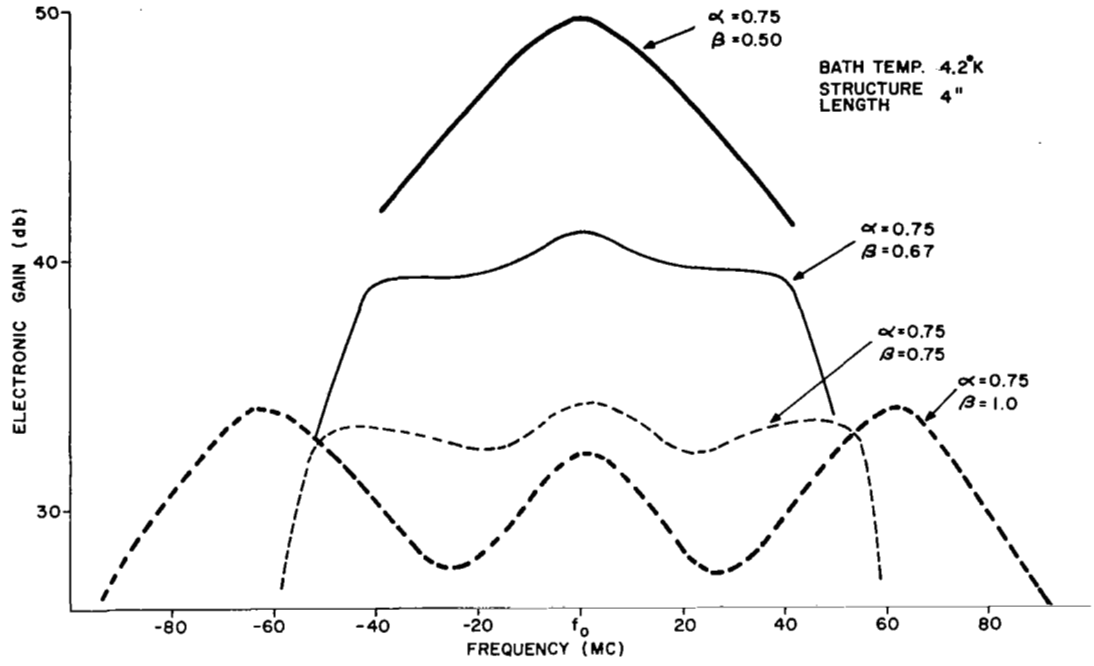

Figure 11. Gain and Bandwidth for $\alpha = 0.75$

Figure 5, coil No. 1 produced field H_1; coils No. 2 and No. 3 were connected in series to produce H_2; and coils No. 4 and No. 5 were used for H_3.

The relative crystal lengths determined by Figures 10 and 11 were used to perform triple-field staggering tests. The first step was to investigate the passband characteristics of each section of the amplifier to determine the shape of the slowing-vs-frequency curve.

2. Passband Characteristics

In order to determine the region of constant slowing and the center frequency of the meander-line circuit, both the paramagnetic absorption and the gain were plotted across the structure band. This region was found to be 150 Mc, centered at 4.0 Gc. Although the amplifier continued to operate well over a 500-Mc tunable range, the region of constant slowing was limited by a number of factors. Chief among them were the dielectric loading, the distance between the

rutile and the ground plane, and the shape and spacing of the ferrite chips used as reverse isolators. In order to utilize simple graphic analysis in approximating the response of the staggered amplifier, the region of constant slowing was employed. Since the peak electronic gain is proportional only to the crystal length, variations in the gain due to changes in signal frequency were neglected. In Figure 12 the paramagnetic absorption of each section has been plotted over the signal band. The resonant frequency of each section has been denoted by arrows on the horizontal scale. Since this curve essentially measures the shape of the slowing-vs-frequency curve, it is clear that only section 3 is slightly frequency dependent near its resonant frequency.

It should be noted that the measurements of each individual section are made under operating conditions; this is accomplished by detuning the crystals not being measured by setting the current in the coils in excess of the value for resonance. This higher current setting assures that no large field gradients will exist and that the insertion losses will be low across the band. The final section of the

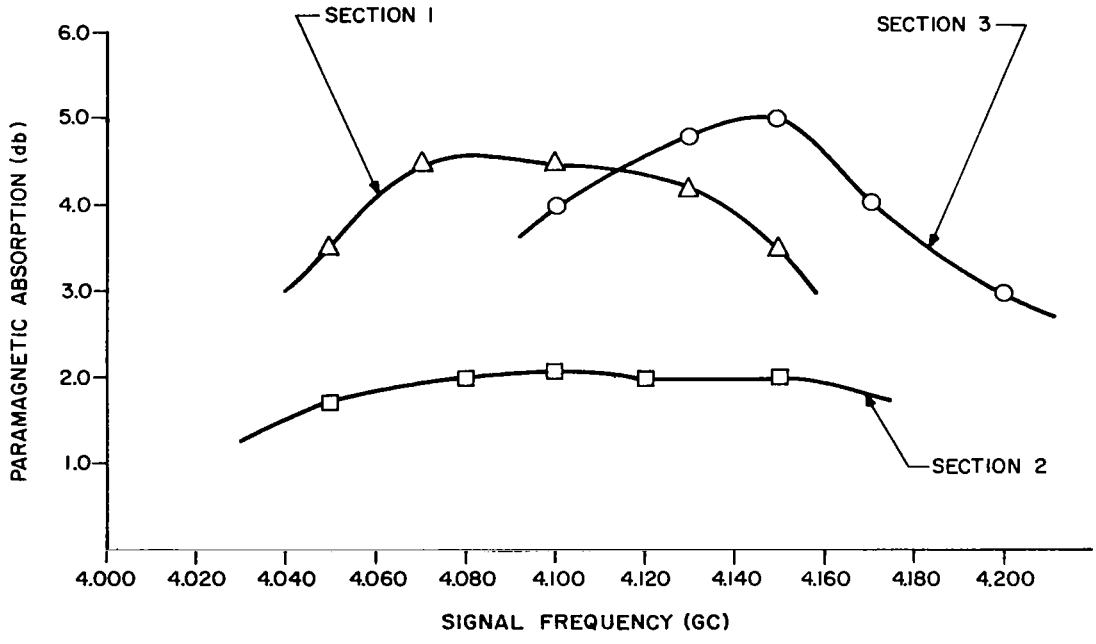

Figure 12. Effects of Summing Magnetic Sections

report shows how it is possible to take advantage of the high gain characteristics of the rutile meander line and achieve broad instantaneous bandwidth by magnetic stagger tuning.

3. Experimental Results

To obtain extremely accurate measurements of the instantaneous bandwidth of the stagger-tuned traveling-wave maser it was decided to measure the electronic gain point-by-point and by tuning the pump frequency at each signal frequency setting. In order to set the magnetic fields at the proper value along the maser structure, the magnetic fields associated with two of the three sections were set to values greater than the resonant value. The receiver was then set to the resonant frequency in question, and the magnet was tuned to the paramagnetic resonance. This magnet power supply was then held fixed and the second and third resonant frequencies were set similarly. The pump Klystron was then turned on. The electronic gain was measured at 10-megacycle intervals across the passband. All the experimental results reported here were obtained in this manner.

In order to determine the pump frequency dispersion necessary for instantaneous bandwidth masers at 4 Gc, the pump frequency was carefully measured across the signal band. Figure 13 shows a curve relating the pump frequency to signal frequency. In the final design of wide-bandwidth masers it will be necessary to supply sufficient pump power to saturate the maser over a range of frequencies on the order of the instantaneous band.

Figure 14 presents the experimental results showing the electronic gain as a function of frequency in the triple-field staggering case. On this curve the individual sections are plotted, and the resultant envelope of the three curves is also recorded. Here again the electronic gain of the individual sections was measured by detuning two of the three crystals as described in the section on the passband characteristics. Clearly the curve is disappointing from a standpoint of wide bandwidth because of the peak on the lower portion of the curve. In order to rectify this situation, the loading of the traveling-wave maser was altered in Section 1

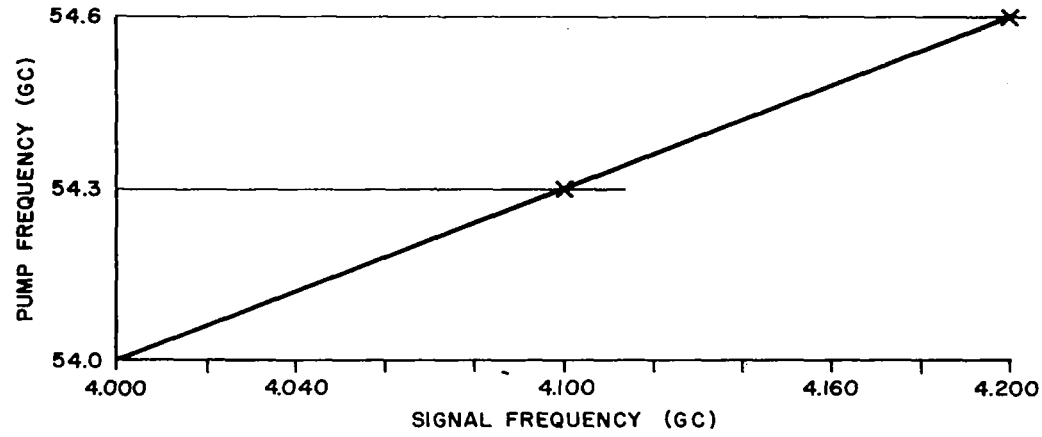

Figure 13. Linear Relationship between Pump and Signal Frequencies

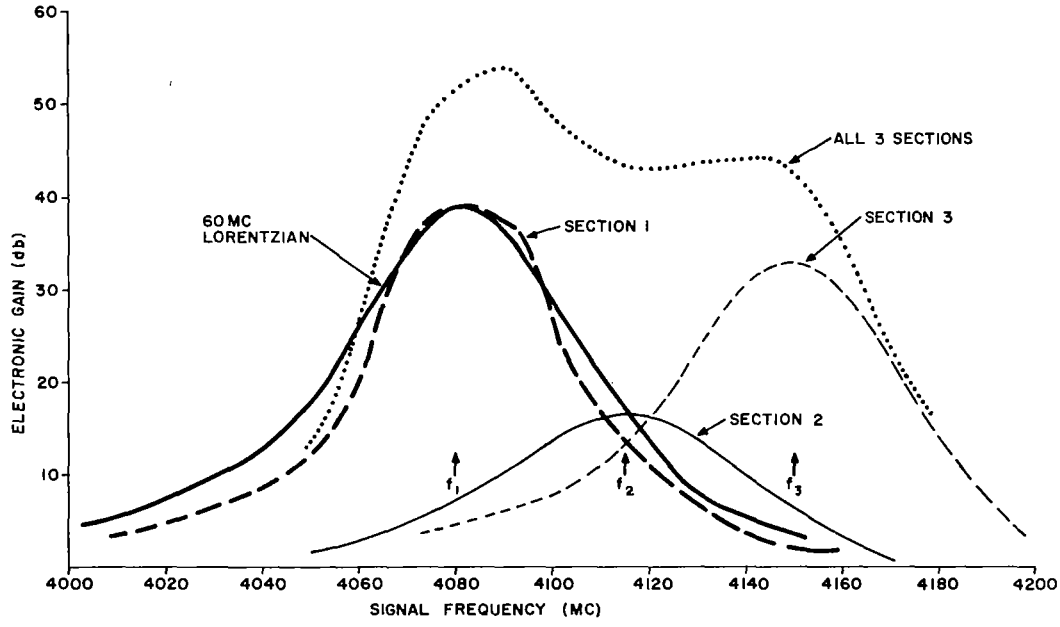

Figure 14. Triple-Field Stagger Tuning by Sections

of the curve to lower the slowing at the lower resonant frequency, f_1. Measurements were then repeated, with the resultant curve shown in Figure 15. Here the electron gain is almost 40 db, although the 3-db bandwidth is approaching 70 megacycles. This represents the maximum performance that has been obtained in the stagger-tuned traveling-wave maser program at the present time. This result approaches the maximum bandwidth that can be obtained with slowing structures that attempt to achieve constant slowing across the signal band.

The three resonant frequencies are indicated by arrows along the horizontal scale (f_1 = 4080 Mc, f_2 = 4115 Mc, f_3 = 4150 Mc). This frequency separation of 35 Mc represents a β value of 0.583, which was shown to be optimum in the graphic analysis of the triple-field staggering case. The experimental values of electronic gain were down 20 per cent from the theoretical value predicted by graphic analysis.

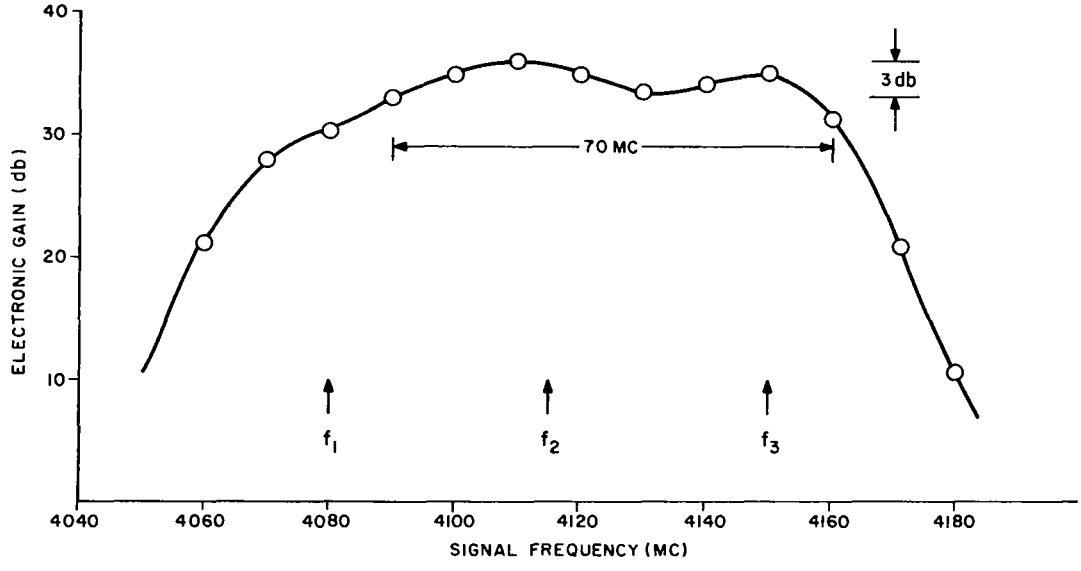

Figure 15. Triple-Field Stagger Tuning Composite

This reduction resulted from the nonuniform gain response of the iron crystals. Since some portions of the crystal were not properly doped, it was felt that a nonuniform inversion ratio vs crystal length had occurred with these crystal samples. The curve shown in Figure 16 demonstrates how the instantaneous bandpass can be shaped by adjusting the individual magnetic fields. The lowest resonant frequency, f_1, was lowered slightly as shown in the figure. As would be expected, the gain at the low-frequency end of the bandpass was increased as the contribution of crystal No. 1 moved to lower frequency. However, the dip in the middle of the passband became deeper since this point in the frequency spectrum loses the sideband contribution of crystal No. 1. It is interesting to note, however, that the bandwidth is increased to 80 Mc, although the dip is now down 4 db from the peak electronic gain.

The insertion losses for a meander-line traveling-wave maser average 4 db per inch. This value results from two major factors: the forward ferrite losses (which average 2 db per inch) and the combined matching and copper losses (which together contribute 2 db per inch). Present VSWR measurements are 1.5 to 1 across the desired bandwidth.

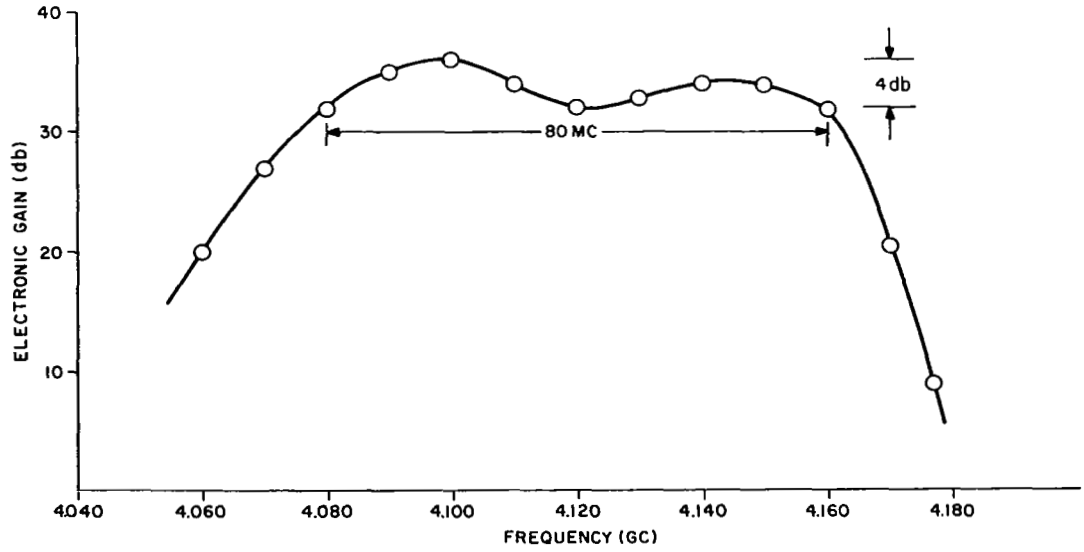

Figure 16. Gain-Bandwidth Trading

Section IV
OPTIMUM STAGGER-TUNED TRAVELING-WAVE MASER

A. INDIVIDUALLY TUNED SECTIONS

In computing the gain/frequency response of stagger-tuned masers, a Lorentzian linewidth of 60 Mc has been used. Experimental results on short pieces of crystal in homogeneous fields have shown good agreement with this assumption. Consequently, success with magnetic stagger tuning over two and three different crystal lengths have been achieved. As mentioned in the previous section, if the instantaneous bandwidth is wide (approximately 100 Mc), it becomes difficult to maintain constant slowing over the entire band without reducing the slowing and severely limiting the electronic gain per inch. Although one may compensate for this by simply adding crystal, a better solution is to achieve higher slowings over larger tuning ranges by adjusting some parameter of the slow-wave circuit such as pitch, copper-to-air ratio or filling factor.

By employing the technique of stagger tuning,[8] large gains may be maintained over a broad range. Briefly, the slowing is optimized or peaked for operation over a narrow band of frequencies for each individual magnetic section of the twm. The resulting gain/frequency response of each crystal length yields a maximum peak gain since the slowing is now optimized over a much narrower range. However, the combination of the sharply tuned meander line and the natural linewidth of the paramagnetic resonance sharpens the gain contribution in the frequency domain. This change can be represented by an effective linewidth which is determined experimentally. This section briefly mentions the design criteria used in developing this concept for a stagger-tuned traveling-wave maser.

The concept utilizes the high gain resulting from a high-slowing, narrow-dispersion meander line. The increase in electronic gain which results from a higher slowing and narrow passband, is demonstrated in Figure 17. As the tunable passband is made narrower, the slowing increases as seen in Figure 17; consequently, extremely high gain can be achieved in short sections.

Since the upper and lower cutoff frequencies of the meander-line circuit extend an octave or more beyond the region of high slowing, it is possible to insert in series a number of high slowing sections. This technique (stagger tuning) allows the designer to achieve a much higher gain per inch over a wider tunable range than would normally be achieved with a constant-slowing flat-dispersion circuit. Since these sections can be peaked at prescribed frequencies, there will result a series of peak gain points centered across the total band which must now be traded for bandwidth. Essentially, two forms of stagger tuning are taking place: stagger tuning of the magnetic susceptibility of the material and stagger tuning of the dispersion curve. The data presented in Figure 18 shows how the slowing structure can be tuned to a particular frequency — in this case, 4.1 Gc; the paramagnetic absorption was used as a measure of this slowing. The data in this curve was taken with a new 4-inch iron-doped rutile crystal which produced 37.5 db/inch electronic

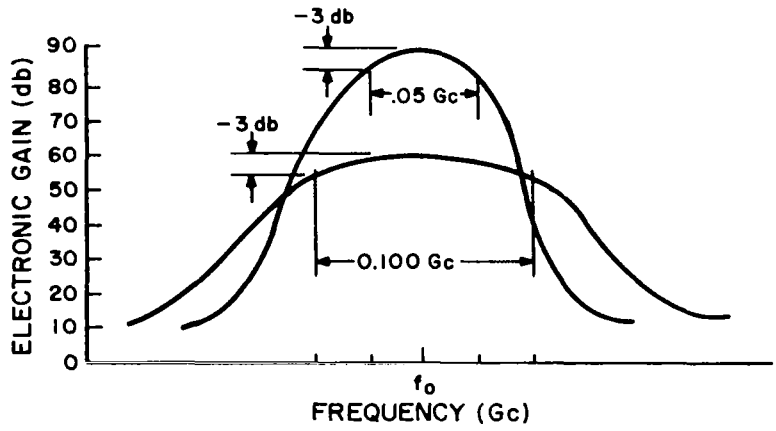

Figure 17. Relationship of Slowing and Dispersion to Gain and Tunability

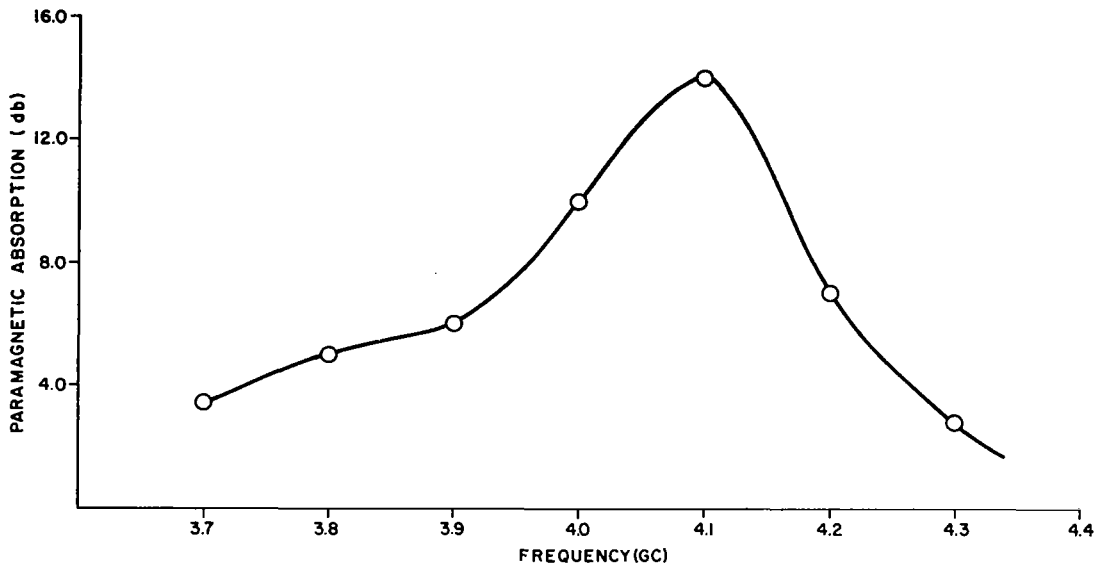

Figure 18. Effects of Large Slowing on Dispersion and Paramagnetic Absorption

gain. The design described in Sections B and C shows how the optimum gain/bandwidth maser at 4.0 Gc can be built using this 4-inch crystal and employing this double-staggering technique. These sections also present the design criteria used in shifting the resonant frequency of the passband.

B. SHIFTING OF PASSBAND RESONANT FREQUENCY

Figure 19 represents a cross-sectional view of a loaded meander-line traveling-wave maser. The dielectric constant of the rutile is represented by ϵ and the effective dielectric constant is given by ϵ'. It can be shown that the center frequency or point of maximum showing for the meander-line structure can be given by:

$$f = \alpha \; d \sqrt{\epsilon'} \qquad (4)$$

This equation in its broadest sense must include 1) the spacing from the rutile to the ground plane (i.e., the thickness of the rutile, a) and 2) the characteristics

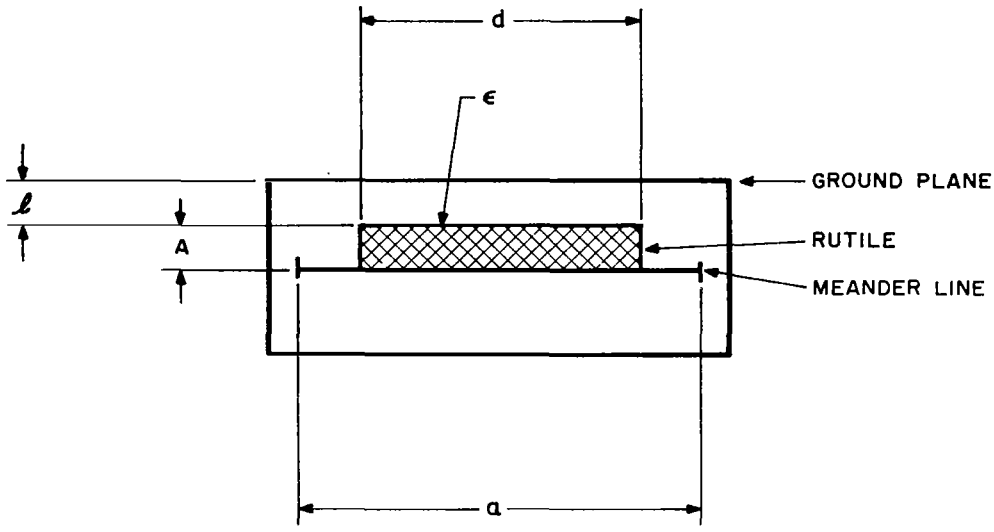

Figure 19. Cross-section of Loaded Meander-Line Traveling-Wave Maser

of the meander line such as copper-to-air ratio, copper width and copper thickness. In addition, the effective dielectric constant, ϵ', is an anisotropic term. A detailed discussion of how these factors affect the loading is beyond the scope of this report but will be discussed in a paper to be published later.

Since the effective dielectric constant is proportional to d, one method of stagger tuning would be to simply change the width of the rutile, d, loading the line. Consequently a series of peak gain points (f, f_1, f_2) are distributed over a broad tunable range.

C. BROADBAND ANALYSIS

Initial experiments with a half-inch piece of iron-doped rutile indicated measured linewidth of 58 Mc when H_{dc} is directed along the c-axis and 70 Mc along the a-axis.

As the length of the crystal sample was increased, this measured linewidth increased to 60 Mc, probably as a result of crystal axis wander and concentration in homogeneity.

A graphic analysis has been carried out based on a 50-Mc linewidth and a Lorentzian line shape for the individual gain contributions. The separation between resonant frequencies has been determined to be 30 Mc instead of 35 Mc as for the 60-Mc case. However, due to the increased slowing and the relatively large magnetic susceptibility for this crystal, a high-performance maser is quite possible. The curve at the top of Figure 20 shows the individual crystal response and the total amplifier response. The frequency separations and the relative gain peaks have been optimized by trial-and-error techniques. Using four crystals and four magnetic fields, a 120-Mc (3 db) response is possible as shown in Figure 20. The four crystals must produce 45, 30, 30 and 45 db, respectively, and must be 30 Mc apart. The remarkable feature of this design is that the total gain required is 150 db which can be produced by only four inches of crystal.

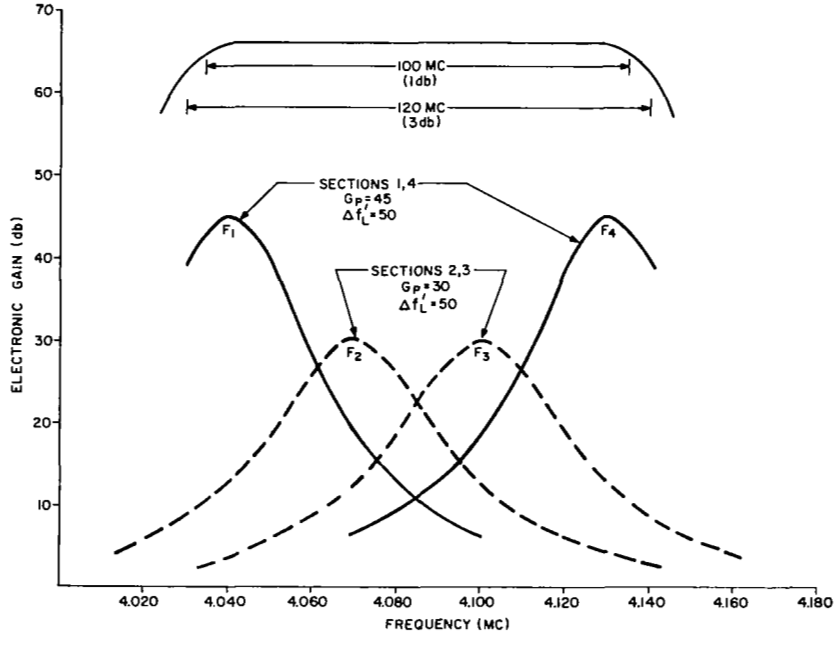

Figure 20. Anticipated Gain-Bandwidth Response for Stagger-Tuned Traveling-Wave Maser (active length is 4 inches)

Table V summarizes the components of this traveling-wave maser amplifier.

TABLE V. OPTIMUM STAGGER-TUNED TRAVELING-WAVE MASER DESIGN

Section	Length (in)	Gain (db)	Frequency (Mc)
1	6/5	45	f_o-45
2	4/5	30	f_o-15
3	4/5	30	f_o+15
4	6/5	45	f_o+45
	4.0	150	

As shown in Figure 19 this maser should produce 66 db of electronic gain over a 100-Mc band measured to the 1-db points.

Section V

CONCLUSIONS

Considering all the major maser materials presently available today, it appears that iron-doped rutile (with its low magnetic field, large linewidth and high inversion ratio) is the best choice for the design of high-gain wide-bandwidth traveling-wave masers. The meander line, with its relatively large region of constant slowing and its low insertion losses in the regions above and below the center of the slowing band, proves an excellent structure with which to couple this high-performance material.

By adding NbTi shielding to the magnet, a compact superconducting magnet has been built and shown to be adequate for accomplishing magnetic stagger tuning. Such a magnet has been operated in a closed-cycle refrigerator with relatively short cool-down times.

By employing triple-field stagger tuning, traveling-wave masers having 70-Mc bandwidth have been constructed. This bandwidth is approaching the maximum attainable with three separate magnetic fields.

This exchange of gain for bandwidth has been shown to be closely correlated to the experimental results and to those predicted by simple theory.

This traveling-wave maser with its wide bandwidth and high gain may be electronically varied; that is, bandwidth may be traded for gain by simply adjusting the magnetic currents through each of the independent windings.

For optimum performance it is necessary to employ stagger-tuning techniques with the slow-wave structure. Based on present experimental evidence concerning

rutiles, inversion ratio, and linewidth, a traveling-wave maser may be constructed with a net gain of 30 db and a 3-db bandwidth of 110 megacycles. The required active material length would be four inches.

REFERENCES

1. R.W. DeGrasse, E.O. Schulz-DuBois, H.E.D. Scovil, "The Three-Level Solid-State Traveling-Wave Maser," BSTJ, 38, 305, (1959).
2. "Operation of Traveling-Wave Masers at Temperatures above 4.2 ^{o}K," final report, prepared for Goddard Space Flight Center, NASA contract NAS 5-3398.
3. F.W. Ostermeyer, "Stagger Tuning of Traveling Wave Masers," Bell Telephone Labs., Murray Hill, N.J., Rept. No. 2, U.S. Army Signal Corps contract DA-36-039-sc-85357, p. 17-24, December 1960.
4. S. Okwit, J.G. Smith, "Traveling-Wave Maser with Instantaneous Bandwidths in Excess of 100 Mc," Proc. IRE, vol. 49, no. 7, p. 1210, July 1961.
5. F. London, "Superfluids," p. 33, Dover, (1960).
6. J.P. McEvoy, Jr., R.F. Decell, "Accurate Low Magnetic Field Measurements on Superconducting Coils," Rev. Scient. Inst., vol. 34, p. 914, (1963).
7. L.C. Morris, D.J. Miller, "Traveling Wave Masers Employing Iron-Doped Rutile," Proc. IEEE, vol. 52, p. 410, (1964).
8. L.C. Morris, D.J. Miller, "A Broad Tunable Bandwidth Traveling Wave Maser," IEEE-MTT, vol. MTT-12, no. 4, pp. 421-428.